Cogent Engineering

ISSN: (Print) (Online) Journal homepage: www.tandfonline.com/journals/oaen20

Investigation of the effectiveness of a stern foil on a patrol boat by experiment and simulation

Muhammad Arif Budiyanto, Muhamad Fuad Syahrudin & Muhammad Aziz Murdianto |

To cite this article: Muhammad Arif Budiyanto, Muhamad Fuad Syahrudin & Muhammad Aziz Murdianto | (2020) Investigation of the effectiveness of a stern foil on a patrol boat by experiment and simulation, Cogent Engineering, 7:1, 1716925, DOI: 10.1080/23311916.2020.1716925

To link to this article: https://doi.org/10.1080/23311916.2020.1716925

Published online: 28 Jan 2020.

cogent engineering

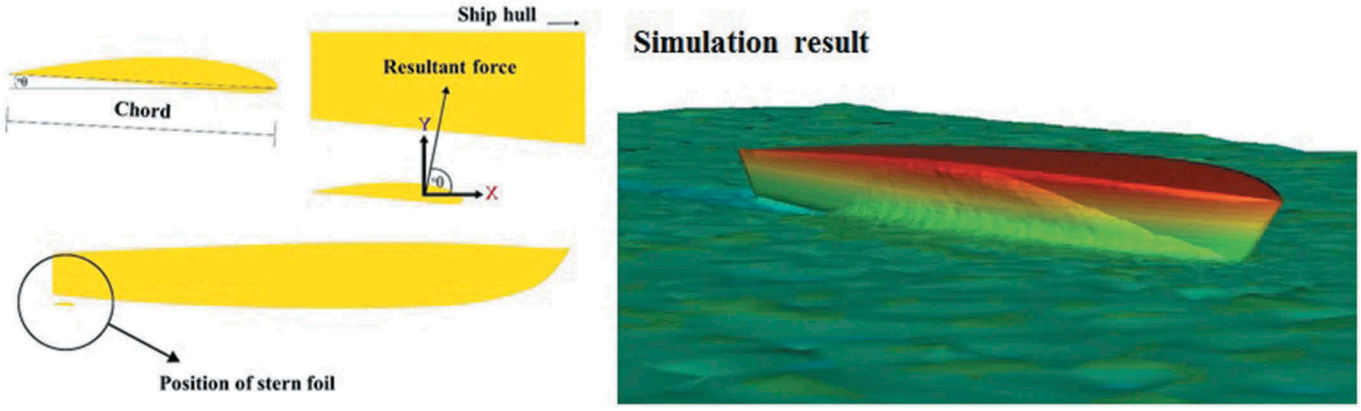

MECHANICAL ENGINEERING | RESEARCH ARTICLE

Investigation of the effectiveness of a stern foil on a patrol boat by experiment and simulation

Muhammad Arif Budiyanto, Muhamad Fuad Syahrudin and Muhammad Aziz Murdianto

Cogent Engineering (2020), 7: 1716925

cogent oa

cogent engineering

MECHANICAL ENGINEERING | RESEARCH ARTICLE

Investigation of the effectiveness of a stern foil on a patrol boat by experiment and simulation

Muhammad Arif Budiyanto[1]*, Muhamad Fuad Syahrudin[1] and Muhammad Aziz Murdianto[1]

Received: 03 July 2019
Accepted: 06 December 2019
First Published: 20 January 2020

*Corresponding author: Muhammad Arif Budiyanto, Mechanical Engineering, Universitas Indonesia, Kampus Baru UI Depok, Jawa Barat 16424, Indonesia
E-mail: arif@eng.ui.ac.id

Featured Application: Application of stern foil in high-speed vessel was effective to reduce ship resistance of 22.3% on the half-full-load condition. Moreover, variation angles of attack of the stern foil reduced a ship resistance with a maximum reduction is 26.7% occurred at Fr 0.9 with angle 0° towards the x-axis.

Reviewing editor:
Duc Pham, University of Birmingham, UK

Additional information is available at the end of the article

Abstract: In the marine industry, specifically fast patrol boats, the important objectives are reducing resistance and improving the efficiency of ships' propulsion systems. The aim of this research was to investigate the application of a stern foil on a patrol boat through experimental and simulation methods. The stern foil used to generate a lift force was an asymmetrical National Advisory Committee for Aeronautics (NACA) foil. In the experiment, the stern foil was installed below the transom of a ship model and positioned parallel to the keel direction (3° towards x-axis). This position created a resultant force, which had an angle to the x-axis. There were variables in this experiment, such as the stern foil application, Froude number (Fr) and hull loads. Those combinations of variables generated sufficient data to analyse the effect of the stern foil working in various conditions. At an optimal load condition (half full load, 2 kg) and Fr 1.1 in the experiment and simulation, the ship model had a resistance reduction of as much as 22.3% and 23.3% in stern foil applications. In addition, with different setups of the stern foil (0° towards the x-axis) in the simulation, a resistance reduction of about 26.7% occurred at Fr 0.9.

Muhammad Arif Budiyanto

ABOUT THE AUTHORS

Muhammad Arif Budiyanto is a faculty member in the Department of Mechanical Engineering, Universitas Indonesia. He completed undergraduate and master's degrees in the Department of Mechanical Engineering, Universitas Indonesia in 2012. He received his doctorate degree in Marine System Engineering from Kyushu University, Japan in 2016. His subject is energy-saving technology in the maritime industry by an experiment and numerical analysis approach.

Muhamad Fuad Syahrudin is undergraduate student in Naval Architecture and Marine Engineering, Universitas Indonesia. His final project is application of stern foil on full draft patrol vessel at high speed condition using towing test method. His work is very significant on this paper to validate the simulation results.

Muhammad Aziz Murdianto is undergraduate student in Naval Architecture and Marine Engineering, Universitas Indonesia. His final project is application of stern foil on full draft patrol vessel at high speed condition using computational fluid dynamics (CFD) methods. His work is very significant on this paper to compute six degrees of freedom on the simulation models.

PUBLIC INTEREST STATEMENT

One of the keys to minimizing a ship's resistance in the high-speed vessel is the application of a stern foil, which affecting trim, reducing wave resistance and generate of lift with a component in the forward direction, so it could produce higher efficiency compared with a planning hull. This paper provides an investigation of application stern foil by the experiment and simulation. Application of stern foil in high-speed vessel was effective to reduce ship resistance of 22.3% on the half-full-load condition. Moreover, variation angles of attack of the stern foil reduced a ship resistance with a maximum reduction is 26.7% occurred at Fr 0.9 with angle 0° towards the x-axis.

Subjects: Mechanical Engineering Design; Ship Operations; Ship Building Technology & Engineering

Keywords: Patrol boat; stern foil; resistance; hull efficiency; simulation

1. Introduction

Nowadays, it is important to consider many points in the ship design process. Moreover, it is often necessary to make improvements or apply new inventions based on a previous design, starting with machining efficiency the impact on production costs. The main factor in any appraisal must be the shape and characteristics of the ship's hull itself, beginning with efficiency through to observation of its wave-making behaviour. The modern era has been rich in new inventions that were intended to increase the efficiency of ships. Engineers tended to focus on developing and modifying the propulsion system and adjusting it to the shape of the hull to which it would be applied (Yun & Bliault, 2012).

Lately, more research has focused on the development and modification of ship performance, and the important objectives will focus on resistance and optimising the efficiency of the ship's propulsion system. Researchers need to keep the main objective under the maintenance, starting with the shape of the hull, wake fraction, interaction between hulls and propulsion systems, right up to the amount of the ship's operating costs (Carlton, 2007; Čerka et al., 2017; Zhang, Ma, & Ji, 2009). The main variables in the ship design process are Length (L), Beam (B), Draught (T), Coefficient block (Cb) and Velocity (V). Changing these variables may affect the optimisation of the design and ship performance, and the results of the calculation of efficiency will depend on the changes to each of them (Edalat & Barzandeh, 2017; Grigoropoulos & Chalkias, 2010).

The preliminary analysis phase and configuration of a ship greatly affect the results of the development and modification of its design, and one of the most important steps is the power prediction analysis. Focusing on ships that have a high Froude number, there are dominant dynamic motions, heave and pitch. These specific motions arise because of dynamic forces, which work directly on the ship, especially in the wetted area. Such motions will work directly to increase the total resistance and fuel consumption of the ship. With the aim of optimising the hydrodynamics and increasing the efficiency of ships, the use of energy-saving technologies has tended to become highly developed (Avci & Barlas, 2019; Huang & Yang, 2016; Zhang, Zhu, & Leng, 2008).

One of the keys to optimising hull design is to minimise resistance by optimising the hull shape (Budiyanto, Novri, Alhamid, & Ardiyansyah, 2019; Campana et al., 2018; Diez, Serani, & Campana, 2017), reducing wave making or wave resistance by using stern flaps (Song, Guo, Gong, Li, & Wang, 2018) and/or applying hydrofoils, which lift the hull above the water's surface and produce higher efficiency compared with a planing hull (Vellinga, 2009). Similar to a hydrofoil, there are interceptors, which cause vortices below the transom area and produce lift (Avci & Barlas, 2019). There is also a submerged hydrofoil that is attached below the hull transom, called a Hull Vane®. The Hull Vane® was invented by Van Oossanen in 1992 and proved capable of reducing ship resistance. Application of the Hull Vane® successfully reduced resistance by approximately 15.3% and 26.5% on a Holland-class, 108-m offshore patrol vessel (OPV) and on a 64-m motor yacht, respectively (Bouckaert et al., 2015; Uithof, Van Oossanen, Moerke, Van Oossanen, & Zaaijer, 2015). On commercial vessels, it reduced resistance by about 5–10%. Furthermore, based on Bouckaert et al. (2015), there was a fuel reduction of 15.3% on a Holland-class, 108-m OPV operating at approximately 17.5 knots.

Unlike a fin stabilizer that reduces the roll motion on a ship when maneuvering (Song et al., 2018), the lift force cause by a Hull Vane® affects the pitch motion and added wave resistance on the ship (Uithof, Hagemeister, Bouckaert, van Oossanen, & Moerke, 2016). Research on the 167-m Ropax vessel Norbank and the 167-m container vessel Rijinborg using a tank test and

computational fluid dynamics (CFD) method concluded that the pitch motion value was reduced by 4.9% and 9.7%, respectively, and additional wave resistance was reduced by 4.46% and 17.3%, respectively, in waves of approximately 2 m in height. In other circumstances, CT enhancement occurred at Fr <0.45 but was reduced at Fr <0.55 (Budiyanto et al., 2019) on an Orela crew boat.

Research on a 1.6-m AMERC (Australian Maritime Engineering Co-operative Research Centre) series #13 patrol vessel showed that Fr 0.5 had the highest resistance reduction of approximately 14.32% followed by 1.53% and 8.05% at Fr 0.6 and 0.7, respectively (Andrews, Avala, Sahoo, & Ramakrishnan, 2015). Moreover, an investigation using CFD simulation compared the application of Hull Vane®, interceptors, trim wedges and ballasting proved the Hull Vane® to have the highest value of resistance reduction, which was approximately 32.4% at Fr 0.35 (Uithof et al., 2016). However, along with increasing Fr, the resistance reduction gap between the Hull Vane® and interceptors, trim wedges and ballasting were diminished because of uniform flows at the end of the transom. Besides, annual fuel savings with the applied Hull Vane® compared to the benchmark with trim wedges and extended benchmark were approximately 15.1%, 8.9% and 6.4% on a 61-m OPV (Hagemeister, Uithof, Bouckaert, & Mikelic, 2017). Research on varieties of AMERC series equipped with Hull Vanes® shows that reductions of about 4%–10%, 18.3%, 21.3% and 12.3% occur on series #3, #4, #8, #11 and #13, respectively, at Fr 0.5–0.7 (Avala, 2017).

The objective of this research was to calculate the ship resistance as the results of applying the stern foil on a patrol boat using an asymmetrical NACA foil to generate a lift force. Displacements were specified for various load conditions, i.e. full, half and empty displacements of the vessel. The stern foil was set parallel to the keel at an angle of 3° counter clockwise towards the x-axis to provide additional translation force on the x-axis. Furthermore, this research carried out an experiment and simulation with Froude numbers ranging between 0.6 and 1.3. These Froude number values were based on the high-speed vessel category meant to indicate speeds in excess of a Froude number value of about 0.4 (Van Oossanen, 1979).

2. Materials and methods

2.1. Mark VI patrol vessel

The Mark VI patrol vessel was the model for this research. It is a high-speed vessel according to its Froude number and unique slender body, and it brings heavy firepower to defend the national territory of the United States Navy. The main dimensions of this ship are as follows: LOA 25.8 m, beam 6.2 m, draught 1.2 m, and service speed 30 knots (HamiltonJet). The following were the main parameters of the model; L/B = 4.162, B/T = 5.167 and Cb = 0.37. The dimensions and lines plan of the model are provided in Table 1 and Figure 1.

The dimensions of a stern foil depend on the Froude number and size of the model, which imposes a limitation on the model's size. Larger values for the model's size are good for stern foil manufacture, but it would be difficult to obtain experimental data at high Froude numbers. On the other hand, a smaller size of the ship model would make stern foil production more difficult.

Table 1. Model's parameters

	Model
Lwl (m)	1
B, beam (m)	0.24
T, draught (m)	0.046
Displacement (kg)	3.25
Cb	0.37

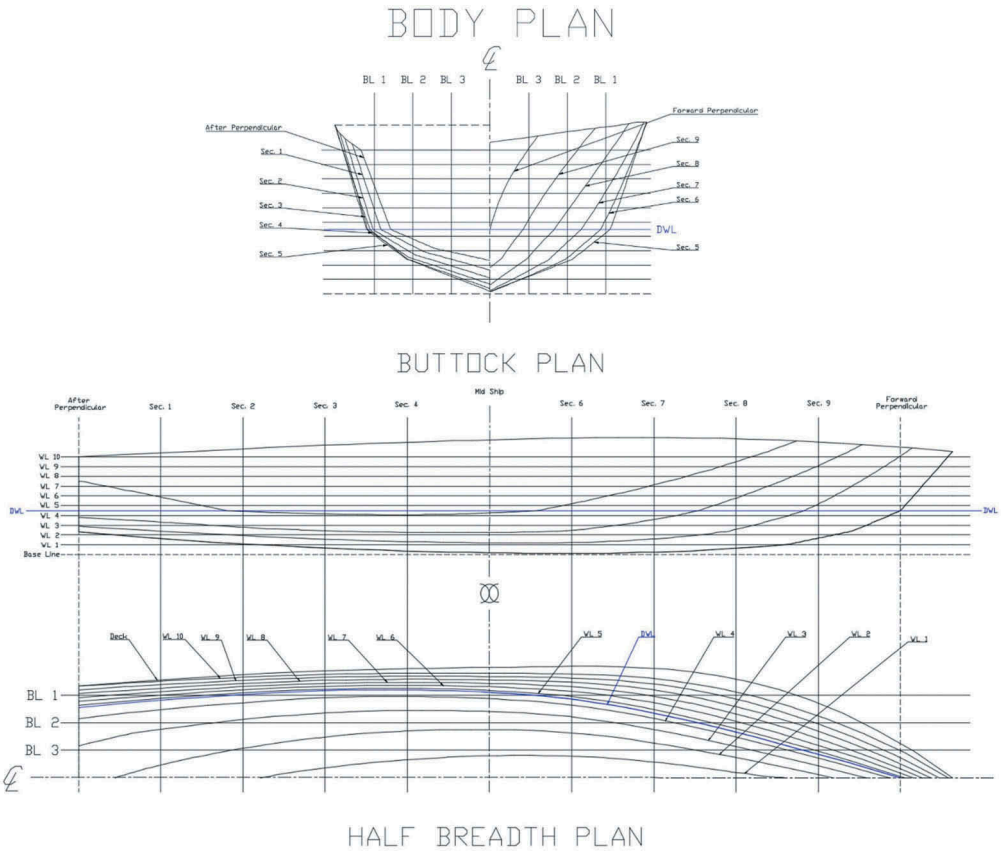

Figure 1. Lines plan of the ship model consist of Body Plan (Front View), Buttock Plan (Side View) and Half Breadth Plan (Top View).

2.2. Stern foil design

Determination of the profile of a stern foil is based on several factors, including the velocity, lift coefficient and the resulting total lift force (Vellinga, 2009). This study used a profile that is classified by the National Advisory Committee for Aeronautics (NACA). The profile of NACA 4412 was chosen because it has a high-lift coefficient at the zero-degree angle of attack (AirfoilTools.com, 2019).

The dimensions of chords and spans must fulfil the needs of the lift force. The lift force required by the stern foil is only 80% of the total displacement of the ship. The width of the ship is one of the references in determining the span dimensions of the stern foil model, so the dimension of the span of the stern foil was set as 20 cm. Whereas the stern foil chord dimension is determined through a trial-and-error process from the calculation of the lift force, this study established the dimension of the chord of the stern foil as 4 cm.

A stern foil is placed below the transom. However, in this experiment the stern foil was also placed parallel to the keel direction. The aim of placing stern foil parallel to the keel is to control the direction of the resultant force, which had an angle θ° to the x-axis, as shown in Figure 2. X and Y are only axis markers, the force created is the lift force which has an angle θ° to the X-axis. The depth of the stern foil was 1.5 times the chord, and it was assumed that the lift force would be affected by the thrust generated from the total-resultant force of the stern foil.

2.3. Experimental procedure

Experiments carried out with two variations of the stern foil conditions, with and without the application of stern foil. The ship model was tested with variation of Froude Number within the range of 0.6–1.3. The ship models were also loaded by variations of range 1–2 kg (empty load and

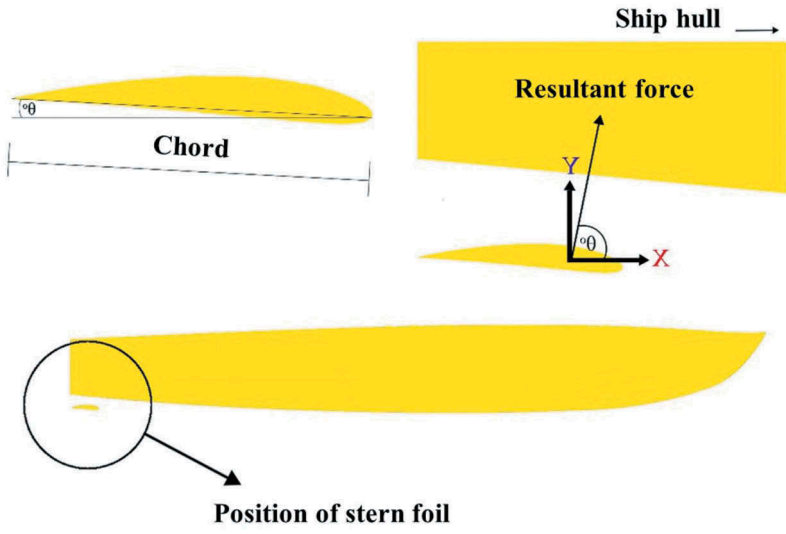

Figure 2. The position of stern foil on ship hulls and its resultant force create a lift force.

half load) to see the changing of the draft of the ship. The combination of variations in stern foil application, Froude Number, and loading generate data to analyse the effect of the stern foil work on the total resistance of the ship with various conditions.

Towing Test method was applied to this experiment with an electric motor that is regulated by AC Voltage Regulator. The electric motor was connected to a rope to the loadcell mounted on the hull of the ship. Assisted with the data acquisition set which consists of a load cell sensor, data recorder, and laptop. The data that was read on the load cell recorded and stored directly on the laptop. By using LabView software, the obtained data is measured by load per time unit. The experiment setup is shown by Figure 3. The obtained data will be processed in accordance with the International Towing Tank Conference (Analysis & Test, 2008). The experiment was carried out on an experimental basin with 25 m x 25 m x 8 m is shown by Figure 4.

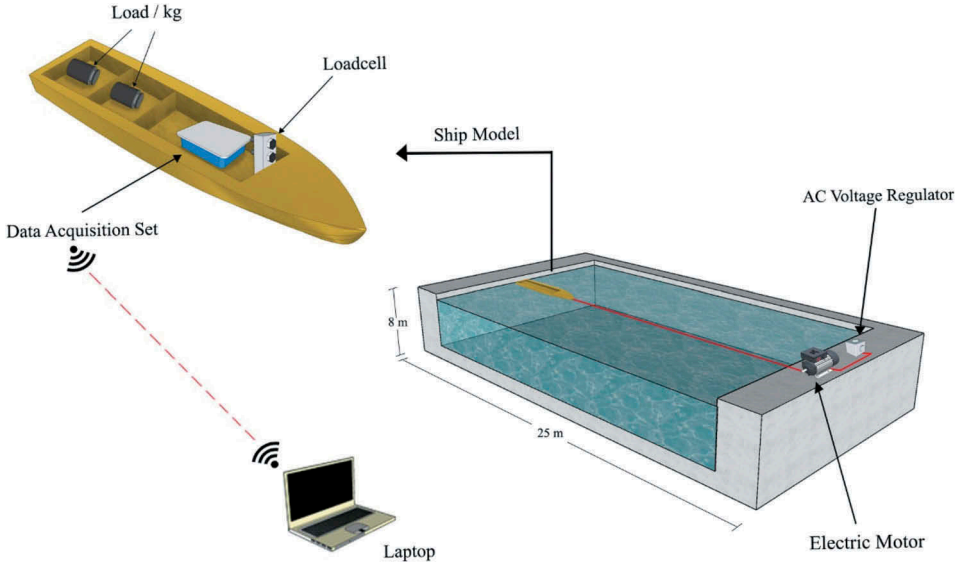

Figure 3. Experimental setup consists of ship models installed with load cell to obtain the data.

Figure 4. Experimental condition on the 25-m water basin, ship models were towed by electric motors.

2.4. CFD simulation

One of the CFD software applications for a single or multiphase flows, according to the required equations, is Ansys Fluent (ANSYS Inc., 2011). This software is used commercially to solve various cases such as ship resistance and maneuverings. Reynold's Averaged Navier–Stokes (RANS) equation, the basic equation used in a CFD program, can be divided into three equations (Zuo, 2015):

$$\frac{D\rho}{Dt}+\rho\frac{\partial U_i}{\partial x_i}=0 \tag{1}$$

$$\rho\frac{\partial U_j}{\partial_t}+\rho U_i\frac{\partial U_j}{\partial x_t}=\frac{\partial P}{\partial x_j}-\frac{\partial \tau_{ij}}{\partial x_i}+\rho g_j \tag{2}$$

$$\rho c_\mu\frac{\partial T}{\partial_t}+\rho c_\mu U_i\frac{\partial T}{\partial x_i}=-P\frac{\partial U_i}{\partial x_t}+\lambda\frac{\partial^2 T}{\partial x_i^2}+\tau_{ij}\frac{\partial U_j}{\partial x_i} \tag{3}$$

Here, Equations (1), (2) and (3) are the continuity equation, momentum equation and energy equation, respectively. Also, ρ, U, P, τ, and g Equation (2) includes the density, momentum, convection surface force, diffusion and mass force. Furthermore, in Equation (3), λ and τ are the heat flux and heat transfer from mechanical energy. For the domain or closure (Danvin, Mathiaud, & Aupoix, 2017), the turbulence model equation uses k-ω SST turbulence model, which is generally used for this scheme, as follows:

$$\frac{\partial_{(\rho k)}}{\partial_t}+\frac{\partial_{(\rho u_j k)}}{\partial x_j}=P-\beta^*\rho\omega k+\frac{\partial}{\partial x_j}\left[\left(\mu+\sigma_k\frac{\rho k}{\omega}\right)\frac{\partial k}{\partial x_j}\right] \tag{4}$$

$$\frac{\partial_{(\rho k)}}{\partial_t}+\frac{\partial_{(\rho u_j \omega)}}{\partial x_j}=\frac{\gamma\omega}{k}P-\beta\rho\omega^2+\frac{\partial}{\partial x_j}\left[\left(\mu+\sigma_\omega\frac{\rho k}{\omega}\right)\frac{\partial k}{\partial x_j}\right]+\frac{\rho\sigma_d}{\omega}\frac{\partial k}{\partial x_j}\frac{\partial \omega}{\partial x_j} \tag{5}$$

In these equations, β, β*, γ, σ_k and σ_d are closure constant coefficients. The variables for this scheme are the Froude number (about 0.6–1.3) and the stern foil, applied or not. In the simulation, the model was at rest and fluids flowed towards it with a constant velocity according to the various Froude numbers specified. The model's movement was restricted in roll, sway, surge and yaw, which basically allowed heave and pitch movements only. To achieve them, the simulation used a user-defined function (UDF) for motion restrictions, as follows:

$$x=x_a\cos(\omega_e t+\varepsilon_{x\varsigma})\ =\ 0 \tag{6}$$

$$y=y_a\cos(\omega_e t+\varepsilon_{y\varsigma})\ =\ 0 \tag{7}$$

$$z=z_a\cos(\omega_e t+\varepsilon_{z\varsigma})\ \neq\ 0 \tag{8}$$

$$\phi = \phi_a \cos(\omega_e t + \varepsilon_{\phi\varsigma}) \; = \; 0 \tag{9}$$

$$\theta = \theta_a \cos(\omega_e t + \varepsilon_{\theta\varsigma}) \neq 0 \tag{10}$$

$$\psi = \psi_a \cos(\omega_e t + \varepsilon_{\psi\varsigma}) \; = \; 0 \tag{11}$$

Here, x, y and z represent the surge, sway and heave, respectively. In addition, ϕ, θ, ψ represent the roll, pitch and yaw, respectively. In this UDF, the mass was specified empty load (1 kg) and half-full load condition (2 kg) thus could be substituted according to the model displacement. IYY is the moment of inertia of a body along the y-axis passing through its centroid, and IXZ is the product of inertia allowing the model to have a pitching motion. Their values are 0.49272 kg·m2 and—0.003444 kg·m2, respectively, and they change depending on the mass applied.

The volume of fluid (VoF) was used to generate a free surface option between fluids. A wall boundary condition was used to simulate or calculate flows near the model for the drag resistance value. Wave and turbulence values were kept low to simulate the calm water condition. The parameters used in Table 2.

The distance for wall-flow was designed to disallow disturbance flow near the model, it is intended that the calculation of ship resistance is not affected by waves caused from outside the model. The main dimensions in the simulation were as follows (ITTC, 2014): The inlet boundary, located at 1-L upstream from the bow of the ship (where L is the ship's length at the water line), was defined as the inlet for fluid that equalled the ship's velocity; The outlet boundary, located at approximately 2-L downstream from the transom of the ship, was also defined as the inlet boundary but at a constant pressure, which allowed incompressible flow in the scheme. Moreover, the bottom and top walls were located at 1-L from the keel and 0.25-L from the deck, respectively. In addition, the side wall was located at 1-L from the longitudinal axis. The dimensions of the simulation are determined based on the practical guidelines of the International

Table 2. Parameter conditions of simulation – main particulars of the ship model

Main Particular of the Ship Model	
Length of Water Line (LWL)	94.66/92.15 (cm)
Wetted Surface Area	1601.55/1349.16 (cm2)
Displacement	2.25/1.25 (kg)
Displacement Volume	3169.89/2208.07 (cm3)
Type of Mesh	Tetrahedral
Domain Physics	Multiphase (Water & Air), K-ω SST Turbulent Model
Physical Parameter	
Pressure	Hydrostatic Pressure
Volume Fraction	Water Volume Fraction
	Mesh Z—axis
Gravity	In Z direction −9.81 m/s2
Boundary Condition	
Inlet	Velocity with defined Froude Number
Outlet	Pressure Outlet (Constant)
Hull and Hull Vane	No Slip Condition
Wall	No Slip Condition (Numerical Beach)
Fluid Properties	
Density of Water	997 kg/m3
Dynamic Viscosity	8.90 × 10 − 4 Pa·s
Surface Tension	0.072 N/m

Towing Tank Conference (ITTC) for ship resistance using CFD. Ship model, strut, foil and wall were defined as the no-slip condition but with an additional numerical beach option for the wall to restrict wave reflection due to boundaries. The numerical beach is to prevent reflections of waves from the outflow boundary into the interior of the domain. The domain showed in Table 3.

The stern foil was applied equally towards the keel using a connecting strut from the ship's leading edge, and the surface distance was 60 mm (1.5 chord of foil) with an angle of attack that was 3° counter clockwise towards the x-axis. The symmetrical foil profile that was used was NACA 0010 with the same chord as the stern foil. The tetrahedral method was used for meshing the ship as shown in Figure 5 and Figure 6. The elements used for the ship were approximately 10 mm with five layers of inflation; those for the strut and stern foil were approximately 1 mm with 25 layers of inflation. A difference in element size and inflation was caused by the part sizes of each model. For accurate

Table 3. Domain of simulation

Domain of simulation	
X (Longitudinal)	4 m
Y (Beam)	2 m
Z (Height)	1.5 m

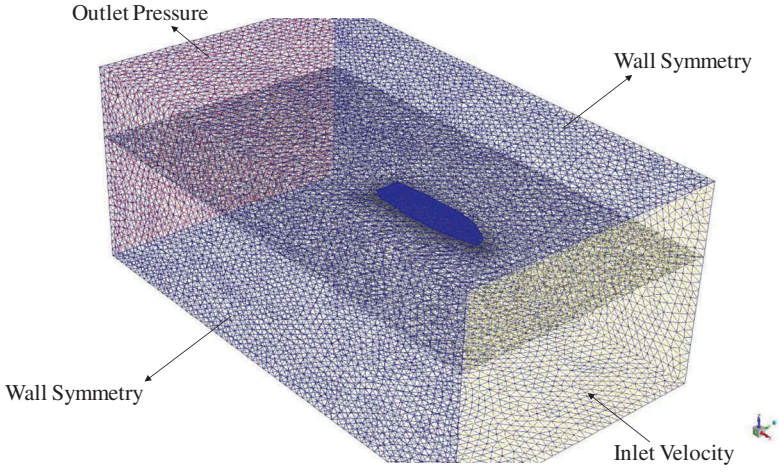

Figure 5. Isometric view of domain.

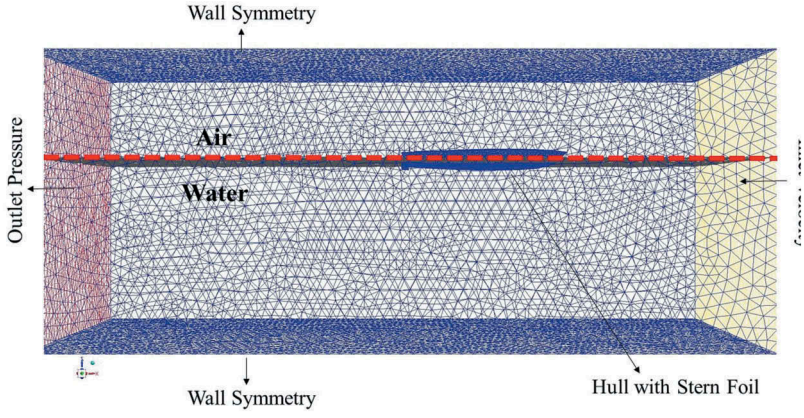

Figure 6. Side view of domain.

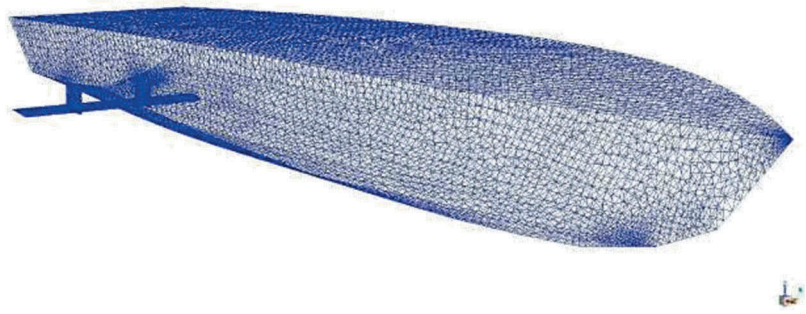

Figure 7. The surface meshing of the ship model using stern foils.

results, inflation was used to calculate the flow that occurred near a wall. Figure 7 below illustrates the surface meshing.

3. Results and discussion

3.1. Experiment

From the results of the experiment using the towing test method, certain velocities were tested on the ship model and some of the total-resistance forces were found. The velocity was obtained when the ship model took a track with a specified distance. The total resistance and Froude number are used in a comparison chart of each variation of the experiment.

Figure 8 shows the results of the towing test experiment on a ship model without the application of a stern foil. We use the trend line method by inputting the data from the experimental results according to the variation of the Froude number. There are three lines that present variations in the loading condition during the experiment. Based on this figure, variations in ship loading show that a higher load generates a higher total resistance experienced by the ship and vice versa (Carlton, 2007). It can be seen that a ship with a half-full load condition (2 kg) experienced a higher

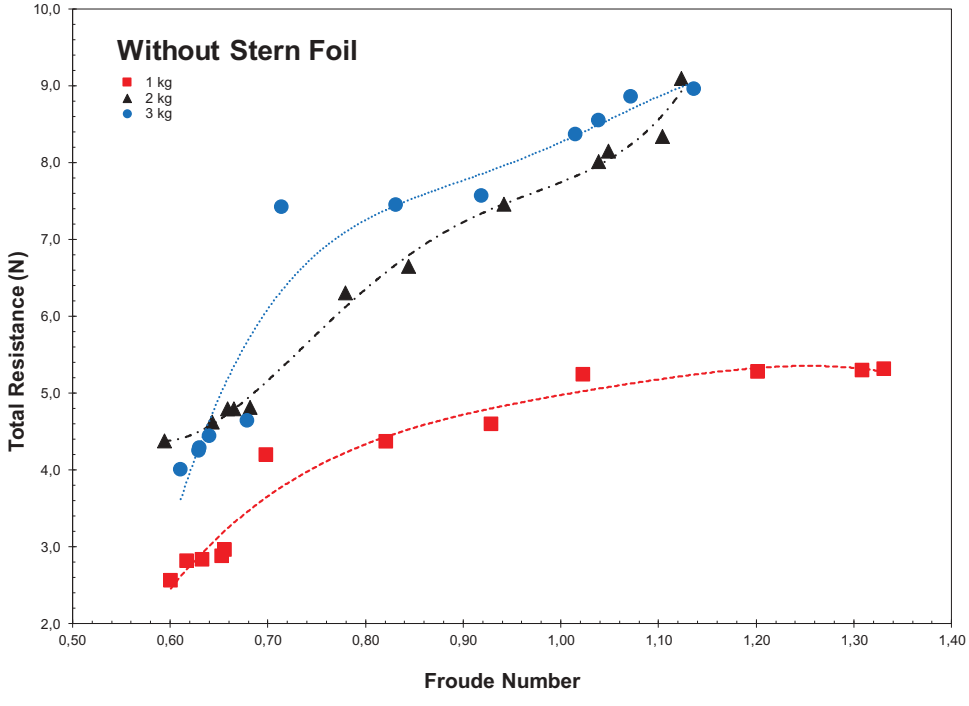

Figure 8. Total ship resistance (N) as a function of Froude number without a stern foil.

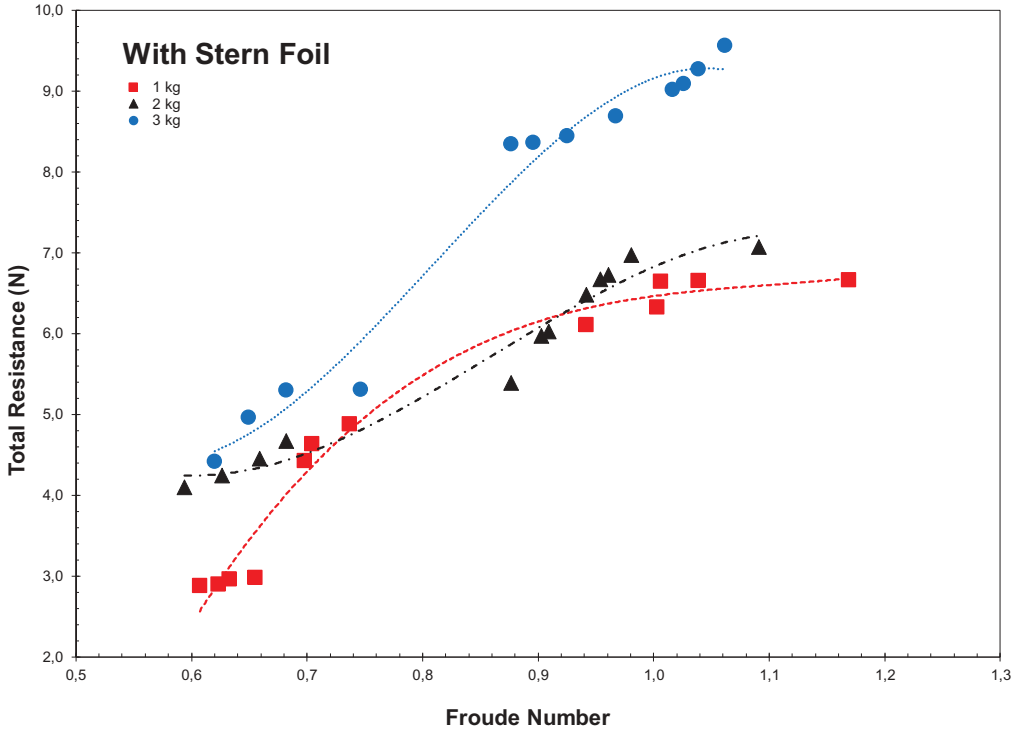

Figure 9. Total ship resistance (N) as a function of Froude number (Fr) with a stern foil.

total resistance compared with one that had a load of 1 kg. The Froude number variations show that with a higher Fr, the total resistance will be even higher, whereas with a low Fr, the total resistance will also below.

Figure 9 shows the results of the towing test experiment on the model ship with a stern foil applied. According to the basic formula for how a hydrofoil works, factors that affect its performance include loading and velocity. In the design process, the optimal performance of a stern foil is found at a load that is 80% of total displacement or about 2.4 kg. After applying the stern foil, it can be shown that the loading conditions empty and half-full load condition (1 and 2 kg) produced a significant increase in resistance. However, in the 2-kg loading condition, the total resistance experienced by the ship model with a stern foil tended to decrease compared with other loading conditions; it could be concluded that the stern foil worked optimally under this condition. According to the loading condition that was set during the design process, the velocity of the ship was also related to the optimal performance of the stern foil. Therefore, if the speed is optimal but loading is not in accordance with the calculation, then the stern foil performance will not work optimally.

Figure 10 is experimental model measurement and shows good improvement with the usage of stern foil under the half-full load condition (2 kg). It is clear that the application of the stern foil reduced the total resistance that occurred in the ship model. This decrease in resistance certainly occurred under the optimal loading condition but was also influenced by the optimal velocity. At the half-full load condition (2 kg) and Fr 1.1, the ship model had an efficiency improvement with the stern foil application that was as much as 22.3%.

3.2. Simulation

Figure 11 compared between both experimental data and simulation data and shows good agreement. It indicates good agreement between the trend lines, with a range of error between 0.178% and 7.161%. This error occurred because of a difference in roughness of the ship model

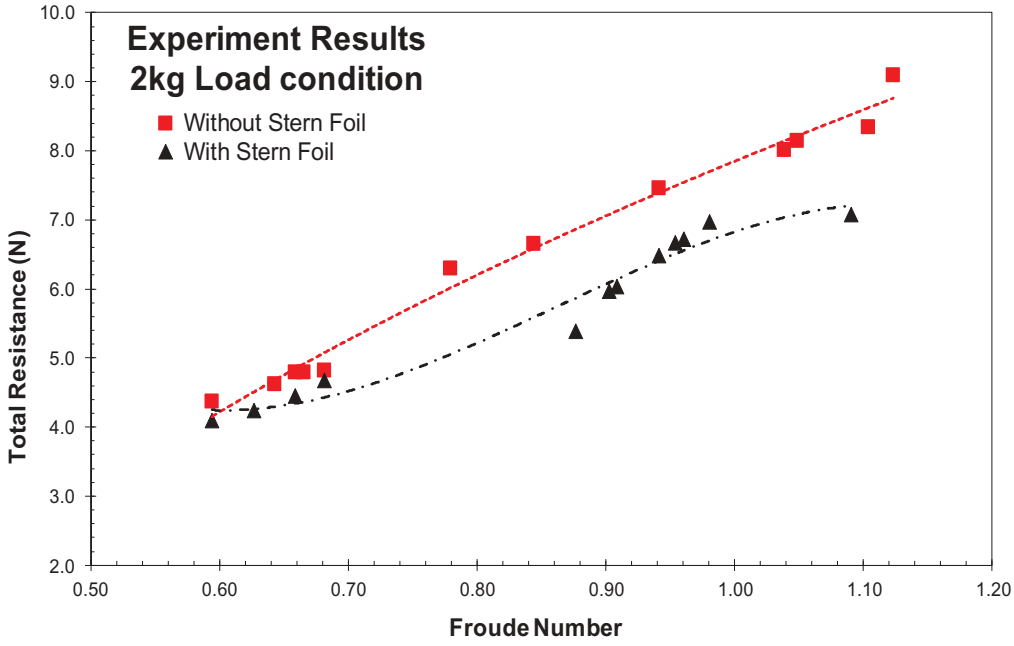

Figure 10. Comparison between the ship model with and without a stern foil.

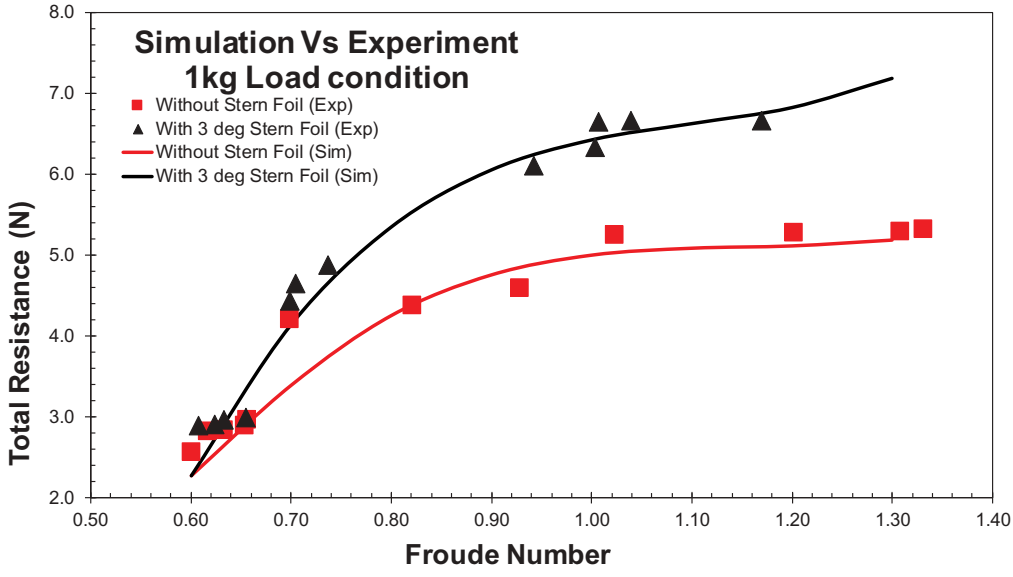

Figure 11. Validation of simulation with experimental results.

between the experiment and simulation. This case was originally unsolved with the simulation method (ITTC–Recommended Procedures and Guidelines, 2011). In the current simulation, a ship model with a half-full load condition (2 kg) was chosen for validation based on the experimental result, which established the effective load for the stern foil.

Figure 12 compared between both experimental data and simulation data and shows good agreement. This figure shows that a reduction of total resistance occurred on the ship model equipped with the stern foil. The simulation in Figure 13 was operated with a 2-kg load, according to the experimental conclusion that the half-full load condition (2 kg) was the optimal load for the stern foil. Total resistance reduction of about 3.2–23.3% occurred compared with the ship model without a stern foil. The highest value for the total resistance reduction (approximately 23.268%)

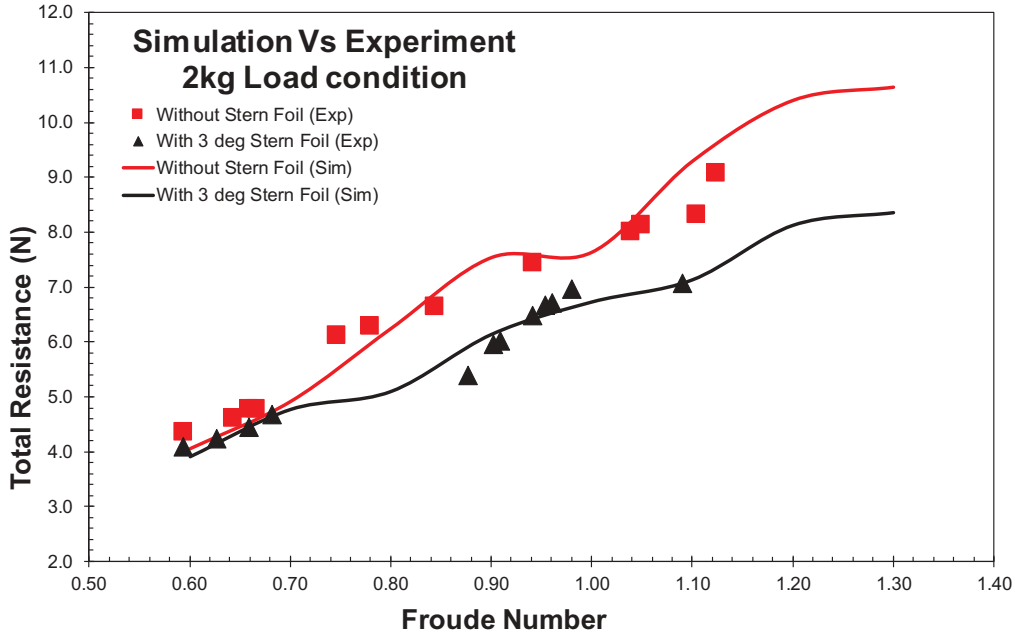

Figure 12. Comparison by simulation under 2 kg with and without a stern foil.

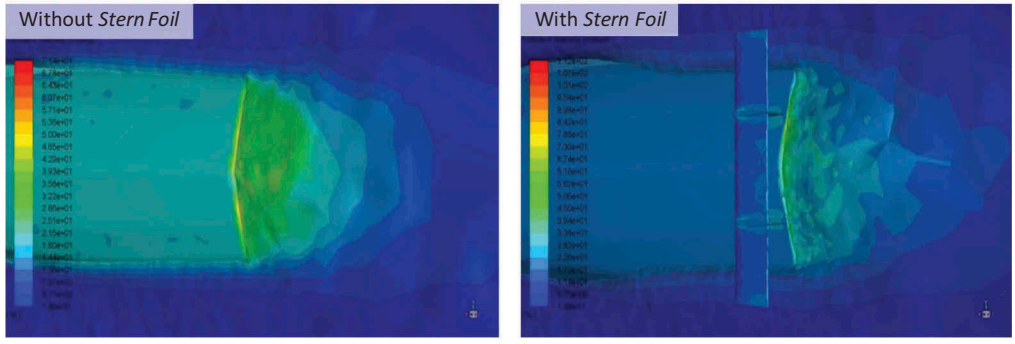

Figure 13. Turbulence intensity near the transom at Fr 1.1 with and without a stern foil.

occurred at Fr 1.1, which corresponded with the experimental result. Furthermore, a total resistance reduction above 20% occurred when the Fr was greater than 1 (23.3%, 21.9% and 21.5% at Fr 1.1, 1.2 and 1.3, respectively). In addition, Figure 13 shows the difference in turbulence intensity that was observed at Fr 1.1 with a 3° angle of attack of the stern foil (parallel to the ship's keel) compared with no stern foil. The amount of turbulence intensity around the stern part according to the colour and scale when not using and using stern foil was about 39.3–42.9% and 22.6%–28.2%, respectively. This difference occured because the stern foil also make the flow after the stern part of model more uniform.

Figure 14 shows comparison of the applied stern foil at angles of attack of about 0° and 3°. It also compares the applied stern foil at an angle of attack of 0° and without a stern foil. As in Figures 12 and 14, the simulation was operated under the same load, specifically 2 kg (half displacement). The graph shows that the differences in stern foil performance were effective at the specified Fr. As in Figure 14, this shows that the stern foil with an angle of attack of 3° was effective at Fr >1. On the other hand, with an angle of attack of 0°, total resistance reduction effectiveness occurred at about Fr <1. Moreover, the total-resistance reduction becomes less effective at Fr ≥1 compared with the stern foil at 3°. On the green line, total resistance reduction occurred at about 7.8–26.7%, with the highest value for reduction occurring at approximately Fr 0.9. It then decreases with increasing values of Fr to about 17.4%, 16.6%, 13.3% and 14.7% at Fr 1,

Figure 14. Effect of angle of attack on the application of stern foil.

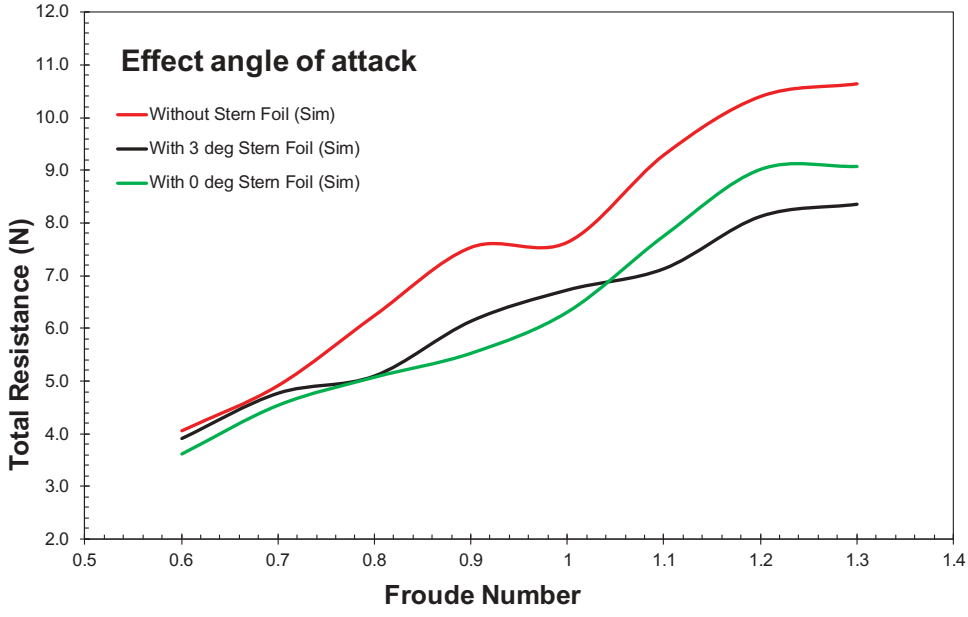

1.1, 1.2 and 1.3, respectively. All the data obtained on simulation method were in a margin of error about 0.178% and 7.161%. The differences occurred because of hull planing, which was becoming higher on the ship model. This caused the angle of attack of the stern foil to become higher, which in turn caused higher resistance compared with 3°.

4. Conclusion

The experiment and simulation on the ship model were based on the ITTC and on CFD simulations using Ansys software. The analysis that was carried out in this study arrived at several conclusions. Successful application of a stern foil on a ship will depend on the conditions. If they are in accordance with the calculations from the design process, the foil will work optimally. From the experiment and simulation, it was found that the application of a stern foil with an asymmetrical profile and an angle of attack parallel to the ship's keel as well as an optimal loading condition (the half-full load, 2 kg) and specific speed (Fr 1.1) will result in a reduction of resistance of 22.3% and 23.3%, respectively. In the 2-kg loading condition, the total resistance experienced by the ship model with a stern foil tended to decrease compared with other loading conditions; it could be concluded that the stern foil worked optimally under this condition. Moreover, with various angles of attack of the stern foil (0° towards the x-axis) in the simulation, a reduction in resistance of about 26.7% occurred at a specific speed (Fr 0.9) but decreased with increasing speed (Fr ≥1). With an angle of attack parallel to the ship's keel at Fr 1.1° and 0° towards the x-axis at Fr 0.9, the turbulence intensity was reduced by at least 7.7%, which made the flow after the stern part of model more uniform. The turbulence intensity's reduction was caused by the reduction of resistance on the ship.

Nomenclature

Abbreviations

NACA	National Advisory Committee for Aeronautics
OPV	Offshore Patrol Vessel
CFD	Computational Fluid Dynamics
AMERC	Australian Maritime Engineering Co-operative Research Centre
RANS	Reynold's Averaged Navier–Stokes
UDF	User-Defined Function
VoF	Volume of Fluid

Roman Symbols	
Lwl	Length waterline
B	Beam
T	Draughts
U	Momentum force
P	Pressure
Fr	Froude Number
Cb	Block Coeeficient
x	Surge motion
y	Sway motion
z	Heavemotion
Greek Symbols	
ρ	Density
λ	Heat flux and heat transfer
ϕ	Roll motion
θ	Pitch motion
ψ	Yaw motion
β, β*, γ, σk and σd	Closure constant coefficients

Acknowledgements
Authors would like to express our gratitude to Directorate Research and Community Engagement (DRPM) Universitas Indonesia in the providing of funding by Q1Q2 2019 research grant Contract No.NKB-0313/UN2.R3.1/HKP.05.00/2019 and PITTA B 2019 research grant [NKB-0761/UN2.R3.1/HKP.05.00/2019].

Funding
This work was supported by the Directorate Research and Community Engagement (DRPM) Universitas Indonesia through Q1Q2 research grant [NKB-0313/UN2.R3.1/HKP.05.00/2019.]; and PITTA B research grant [NKB-0761/UN2.R3.1/HKP.05.00/2019].

Author details
Muhammad Arif Budiyanto[1]
E-mail: arif@eng.ui.ac.id
ORCID ID: http://orcid.org/0000-0001-8118-7521
Muhamad Fuad Syahrudin[1]
E-mail: fuadsyahrudin234@gmail.com
Muhammad Aziz Murdianto[1]
E-mail: muhammad.aziz51@ui.ac.id
[1] Department of Mechanical Engineering, Universitas Indonesia, Kampus Baru UI Depok, Jawa Barat, 16424, Indonesia.

Citation information
Cite this article as: Investigation of the effectiveness of a stern foil on a patrol boat by experiment and simulation, Muhammad Arif Budiyanto, Muhamad Fuad Syahrudin & Muhammad Aziz Murdianto, *Cogent Engineering* (2020), 7: 1716925.

Cover image
Source: Author.

References

AirfoilTools.com. (2019). NACA 4412. Retrieved from http://airfoiltools.com/airfoil/details?airfoil=naca4412-il

Analysis, D., & Test, R. (2008). ITTC – Recommended procedures and guidelines. *International Towing Tank Conference*.7.5-02-03-02.

Andrews, I., Avala, V. K., Sahoo, P., & Ramakrishnan, S. (2015, October). Resistance characteristics for high-speed hull forms with vanes. *13th International Conference on Fast Sea Transportation, FAST '2015*. (pp. 5–10), Washington DC, USA.

ANSYS Inc.. (2011). *Tutorial : Heave and pitch simulation of ship hull moving through head sea waves introduction setup and solution preparation* (pp. 1–27). ANSYS FLUENT 13.0 Tutorial Guide.

Avala, V. K. (2017, May). *CFD analysis of resistance characteristics of high-speed displacement hull forms fitted with hull vane*. Florida Institute of Technology.

Avci, A. G., & Barlas, B. (2019). An experimental investigation of interceptors for a high speed hull. *International Journal of Naval Architecture and Ocean Engineering*, *11*(1), 256–273. doi:10.1016/j.ijnaoe.2018.05.001

Bouckaert, B., Uithof, K., van Oossanen, P., Moerke, N., Nienhuis, B., & van Bergen, J. (2015). A life-cycle cost analysis of the application of a hull vane ® to an offshore patrol vessel. *1*(V), 10. In FAST 2015, Washington DC, USA.

Budiyanto, M. A., Novri, J., Alhamid, M. I., & Ardiyansyah, (2019). Analysis of convergent and divergent-convergent nozzle of waterjet propulsion by CFD simulation. *AIP Conference Proceedings*. doi:10.1063/1.5086613

Campana, E. F., Diez, M., Liuzzi, G., Lucidi, S., Pellegrini, R., Piccialli, V., … Serani, A. (2018). A multi-objective DIRECT algorithm for ship hull optimization. *Computational Optimization and*

Applications, *71*(1), 53–72. doi:10.1007/s10589-017-9955-0

Carlton, J. (2007). *Ship resistance and propulsion*. Butterworth-Heinemann, 3rd edition (October 30, 2012). ISBN-13: 978-0080971230

Čerka, J., Mickevičienė, R., Ašmontas, Z., Norkevičius, L., Žapnickas, T., Djačkov, V., & Zhou, P. (2017). Optimization of the research vessel hull form by using numerical simulaton. *Ocean Engineering*, *139* (October 2016), 33–38. doi:10.1016/j.oceaneng.2017.04.040

Danvin, F., Mathiaud, J., & Aupoix, B. (2017, September). *Study on k- w shear stress transport model corrections applied to rough wall turbulent hypersonic boundary layers*. 7th european conference for aeronautics and space sciences (eucass).DOI: 10.13009/EUCASS2017-604

Diez, M., Serani, A., & Campana, E. F. (2017). CFD-based stochastic optimization of a destroyer hull form for realistic ocean operations. 14th Int. Conf. Fast Sea Transp. - FAST 2017 (pp. 1–9), Nantes, France.

Edalat, P., & Barzandeh, A. (2017). Fuel efficiency optimization of tanker with focus on hull parameters. *Journal of Ocean Engineering and Science*, *2*(2), 76–82. doi:10.1016/j.joes.2017.03.002

Grigoropoulos, G. J., & Chalkias, D. S. (2010). Hull-form optimization in calm and rough water. *CAD Computer-aided Design*, *42*(11), 977–984. doi:10.1016/j.cad.2009.11.004

Hagemeister, N., Uithof, K., Bouckaert, B., & Mikelic, A. (2017). *HULL VANE ® VERSUS LENGTHENING A comparison between four alternatives for a 61m OPV*.14th Int. Conf. Fast Sea Transp. - FAST 2017 (pp. 1–11), Nantes, France.

HamiltonJet. *'MK VI coastal riverine force' JetBrief* (Vol. 467, pp. 651). Woodinville WA, USA: HamiltonJet INC.

Huang, F., & Yang, C. (2016). Hull form optimization of a cargo ship for reduced drag. *Journal of Hydrodynamics*, *28*(2), 173–183. doi:10.1016/S1001-6058(16)60619-4

ITTC. (2014). Practical guidelines for ship resistance CFD. ITTC – Recomm. Proced. Guidel. 27th (pp. 1–9). International Towing Tank Conference 7.5-03-03-01

ITTC - Recommended Procedures and Guidelines. (2011) . Practical guidelines for ship CFD. 26th Int. Towing Tank Conf. International Towing Tank Conference 7.5-02-03

Song, K. W., Guo, C. Y., Gong, J., Li, P., & Wang, L. Z. (2018). Influence of interceptors, stern flaps, and their combinations on the hydrodynamic performance of a deep-vee ship. *Ocean Engineering*, *170* (January), 306–320. doi:10.1016/j.oceaneng.2018.10.048

Uithof, K., et al. (2016). A systematic comparison of the influence of the hull vane ®, Inter- Ceptors, trim wedges, and ballasting on the performance of the 50M Amecrc Series # 13 patrol vessel. (June), 15–16. doi:10.1007/978-1-4939-6337-9_2.

Uithof, K., Hagemeister, N., Bouckaert, B., van Oossanen, P. G., & Moerke, N. (2016). The effects of the hull vane on ship motions of ferries and ropax vessels warsh. *Adv. Technol. Nav. Des. Constr. Oper*, (May), 7.

Uithof, K., Van Oossanen, P., Moerke, N., Van Oossanen, P. G., & Zaaijer, K. S. (2015). *An update on the development of the hull vane ®*.

Van Oossanen, P. (1979, November 5-7). Resistance prediction of small high speed displacement vessels.Pdf. *In Symposium on "The Impact of 200 Mile Economic Zones" Organized by the Royal Institution of Naval Architects (Australian Branch) and the Institute of Marine Engineers* (pp. 1–12). Sydney, Australia.

Vellinga, R. (2009, January). *Hydrofoils design built fly* (1st ed.). Peacock Hill Publishing. ISBN-13: 978-0982236116

Yun, L., & Bliault, A. (2012). *High performance marine vessels*. Liang Yun • Alan Bliault.pdf. London, UK: Springer.

Zhang, B. J., Ma, K., & Ji, Z. S. (2009). The optimization of the hull form with the minimum wave making resistance based on rankine source method. *Journal of Hydrodynamics*, *21*(2), 277–284. doi:10.1016/S1001-6058(08)60146-8

Zhang, P., Zhu, D. X., & Leng, W. H. (2008). Parametric approach to design of hull forms. *Journal of Hydrodynamics*, *20*(6), 804–810. doi:10.1016/S1001-6058(09)60019-6

Zuo, W. (2015). *Introduction of computational fluids dynamics*. FAU Erlangen-Nürnberg JASS 05, St. Petersburg.

Cogent Engineering **(ISSN: 2331-1916) is published by Cogent OA, part of Taylor & Francis Group.**